Supplementary Appendix: Prioritizing COVID-19 vaccination in changing social and epidemiological landscapes

Peter Jentsch[1,2], **Madhur Anand**[1], **and Chris T. Bauch**[2,*]

[1]Department of Applied Mathematics, University of Waterloo, Waterloo, Ontario, Canada; [2]School of Environmental Sciences, University of Guelph, Guelph, Ontario, Canada; *cbauch@uwaterloo.ca

Supplementary Methods

Model Equations. Transmission dynamics are given by an SEAIR model, modified to take population adherence to NPIs and school/workplace closure into account, and divided into age classes $i \in [1, 16]$, where each age class contains a 5 year cohort, except for the oldest age group which comprises the ages 75 and over. The model equations are:

$$\frac{dS_i^1}{dt} = -r\rho_i \left[1 + s\sin\left(\frac{2\pi}{365}(t-\phi) - \frac{\pi}{2}\right)\right] S_i^1 \sum_{j=1}^{16} C_{ij}(t)\left(\frac{I_{s_j} + I_{a_j}}{N_j}\right) \quad [1]$$

$$\frac{dS_i^2}{dt} = -r\rho_i \left[1 + s\sin\left(\frac{2\pi}{365}(t-\phi) - \frac{\pi}{2}\right)\right] S_i^2 \sum_{j=1}^{16} C_{ij}(t)\left(\frac{I_{s_j} + I_{a_j}}{N_j}\right) \quad [2]$$

$$\frac{dS_i^3}{dt} = -r\rho_i \left[1 + s\sin\left(\frac{2\pi}{365}(t-\phi) - \frac{\pi}{2}\right)\right] S_i^3 \sum_{j=1}^{16} C_{ij}(t)\left(\frac{I_{s_j} + I_{a_j}}{N_j}\right) \quad [3]$$

$$\frac{dE_i}{dt} = r_i \left[1 + s\sin\left(\frac{2\pi}{365}(t-\phi) - \frac{\pi}{2}\right)\right] (S_i^1 + S_i^2 + S_i^3) \sum_{j=1}^{16} C_{ij}(t)\left(\frac{I_{s_j} + I_{a_j}}{N_j}\right) - \sigma E_i \quad [4]$$

$$\frac{dI_{a_i}}{dt} = \eta\sigma E_i - \gamma_a I_{a_i} \quad [5]$$

$$\frac{dI_{s_i}}{dt} = (1-\eta)\sigma E_i - \gamma_s I_{s_i} \quad [6]$$

$$\frac{dR_i}{dt} = \gamma_a I_{a_i} + \gamma_s I_{s_i} \quad [7]$$

$$\frac{dD_i}{dt} = \Omega(D(t)) \quad [8]$$

Parameter values are defined in Table S1. The vaccination dynamics are an impulsive process applied each day, described below. S_i^1 is the number of unvaccinated susceptible individuals in age group i, S_i^2 is the number of susceptible individuals in age group i who have been vaccinated once (without being immunized), and S_i^3 is the number of susceptible individuals in age group i who have been vaccinated twice while remaining susceptible. $E_i(t)$ is the number of exposed but not infectious individuals in age group i. $I_{a_i}(t)$ is the number of asymptomatic infectious individuals in age group i and $I_{s_i}(t)$ is the number of symptomatic infectious individuals in age group i. $R_i(t)$ is the number of Removed (recovered, vaccinated, and deceased) individuals in compartment i.

The variable $D(t) \in [0, 1]$ in the model equation $dD(t)/dt = \Omega(D(t))$ represents the public health authority's reaction to the prevalence of ascertained cases and it evolves according to:

$$\Omega(D(t)) = \begin{cases} k_1(1 - D(t)) & \sum_{i=1}^{16} \alpha_i(I_{a_i} + I_{s_i}) > T \\ -k_2 D(t) & \sum_{i=1}^{16} \alpha_i(I_{a_i} + I_{s_i}) \leq T \end{cases} \quad [9]$$

This represents closure being eventually triggered when ascertained cases exceed a threshold T, and being lifted when cases drop below that threshold again.

The proportion x of individuals who practice NPIs such as mask wearing, handwashing, and physical distancing, starts off at $x(0) = 0.01$ and evolves as:

$$\frac{dx}{dt} = \kappa x(1-x)\left(\sum_{i=1}^{16} \alpha_i(I_{a_i} + I_{s_i}) - cx\right) + p_{ul}(1 - 2x) \quad [10]$$

where κ is the social learning rate, c is the incentive to not practice NPIs, and α_i is the fraction of total cases $(I_a + I_s)$ that are reported, also known as the ascertainment rate. The p_{ul} term is a phenomenological term that represents

the effects of social heterogeneity and influence from external populations that prevents the system from remaining arbitrarily close to $x = 0$ or $x = 1$ for unrealistic periods of time. These equations describe a population where individual sample other individuals at some time rate and switch between adherence and non-adherence to NPIs with a probability proportional to the expected gain in utility $\sum_{i=1}^{16} \alpha_i(I_{a_i} + I_{s_i}) - cx$. We refer the reader to existing literature for details on the derivation of this equation (1–5).

$C_{ij}(t)$ is the average number of contacts per day and consists of contacts at workplaces, schools, households, and other locations, which vary depending on government shutdown policies as well as indivdual adherence to NPIs like physical distancing and mask use:

$$C_{ij}(t) \quad = \quad C_{ij}^{W}(t) + C_{ij}^{S}(t) + (1 - \epsilon_P x)(\overline{C}_{ij}^{O} + \overline{C}_{ij}^{H}) \qquad [11]$$

The contacts in each of the aforementioned places can vary as follows. At workplaces, which can be closed by public health authorities:

$$C_{ij}^{W}(t,x) = \begin{cases} (1-\epsilon_W)\overline{C}_{ij}^{W} & t > t_{close}, t < t_{open}^{w} \\ \overline{C}_{ij}^{W} & t < t_{close}^{w} \\ (1 - D(t)(1-\epsilon_W))\overline{C}_{ij}^{W} & t > t_{open}^{w} \end{cases} \qquad [12]$$

where $\overline{C}_{ij}^{W}$ is the normal (non-pandemic) number of contact-hours per day between individuals of age i and j at the workplace (6), and $\overline{C}_{ij}^{W}(1 - D(t)\epsilon_P)$ is the reduced rate under workplace closure efficacy $0 < \epsilon_W < 1$ and closure level $D(t)$. Lower than perfect efficacy may stem either from occasional use of workplace for critical needs or non-authorized access, workplaces that remain open because they provide essential services, etc. t_{close}^{W} and t_{open}^{W} are the times of closing and re-opening workplaces, respectively. Similarly, for schools we have:

$$C_{ij}^{S}(t) = \begin{cases} 0 & t > t_{close}^{s}, t < t_{open}^{s} \\ \overline{C}_{ij}^{S} & t < t_{close}^{s} \\ (1 - D(t))\overline{C}_{ij}^{S} & t > t_{open}^{s} \end{cases} \qquad [13]$$

All other places of exposure are governed by social processes with imperfect ability of public health authorities to enforce mandages, and hence are governed by voluntary population adherence to NPIs such as mask use and physical distancing as per the $\epsilon_P x(t)$ term in the equation, where ϵ_P is efficacy of individual adoption of NPIs. In principle, contact hours spent at home should increase as workplaces and schools are closed, but we assume that infection probabilities will saturate rapidly with contact hours in the home. Each of the conditional functions in equations (12,13), are represented in the model as a smoothed step function with a steep slope, and we restrict them between 0 and 1 if the smoothing process would cause the closure level $D(t)$ to exceed 1.0.

Vaccination process. Each day, the total number of individuals vaccinated is equal to $\sum_{i=1}^{16} \phi_i \frac{S_i(t)}{N_i}$, and the number of individuals immunized is $\sum_{i=1}^{16} v_i \frac{S_i(t)}{N_i}$ on account of imperfect vaccination. The factor $\frac{S_i(t)}{N_i}$ represents vaccination of each person with equal probability, so the probability of vaccinating a susceptible person decreases with the fraction of susceptible individuals remaining in the population. If there are less than ϕ_i individuals in group S_i^1, then the remainder of the vaccine is spread evenly among the remaining non-vaccinated groups. Individuals who are vaccinated but not immunized due to imperfect efficacy are moved to the corresponding S_i^2. If there are remaining vaccines after all individuals in S^1 (for $i = 1..16$) have been vaccinated, then the same process is conducted on S_i^2. We assume that a course of vaccination will not be administered to a person more than twice.

Case under-ascertainment. Case under-ascertainment is represented by the variables $\alpha_i, i \in [1, 16]$, which are interpolated from eight variables $\alpha'_i, i \in [1, 8]$ used to fit the ascertainment, where each α'_i corresponds to two consecutive age groups. We use quadratic interpolation functions to interpolate each α'_i to the respective α_i, to reduce the dimensionality of the parameter space. We multiply the infections in each age group i by the corresponding α_i after the simulation is finished.

Baseline transmission rate. We can compute r as a function of the next-generation matrix, $M = -\Theta\Sigma^{-1}$ (7), where Θ and Σ are defined as in equations 14,15, and so M is a function of $R_0, \sigma, \gamma_a, \gamma_s, \eta, C(t)$, and N. These matrices come from the rate at which infected individuals enter and leave the infection compartments when the system is linearized about the $I_a = 0, I_s = 0$ equilibrium. The basic reproduction ratio, R_0, of the infection is the spectral radius of M,

written $\rho(M)$. We can pull r out of this expression and write r in terms of the other parameters: $r = \frac{R_0}{\rho(M)}$.

$$\Theta = \begin{bmatrix} 0 & \dots & 0 & \frac{rC_{1,1}(0)N_1}{N_1} & \dots & \frac{rC_{1,n}(0)N_1}{N_n} & \frac{rC_{1,1}(0)N_1}{N_1} & \dots & \frac{rC_{1,n}(0)N_1}{N_n} \\ \vdots & \ddots & \vdots & \vdots & \vdots & \ddots & \vdots & \ddots & \vdots \\ 0 & \dots & 0 & \frac{rC_{1,n}(0)N_n}{N_1} & \dots & \frac{rC_{n,n}(0)N_n}{N_n} & \frac{rC_{1,n}(0)N_n}{N_1} & \dots & \frac{rC_{n,n}(0)N_n}{N_n} \\ 0 & \dots & 0 & 0 & \dots & 0 & 0 & \dots & 0 \\ \vdots & \ddots & \vdots & \vdots & \ddots & \vdots & \vdots & \ddots & \vdots \\ 0 & \dots & 0 & 0 & \dots & 0 & 0 & \dots & 0 \\ 0 & \dots & 0 & 0 & \dots & 0 & 0 & \dots & 0 \\ \vdots & \ddots & \vdots & \vdots & \ddots & \vdots & \vdots & 0 & \vdots \\ 0 & \dots & 0 & 0 & \dots & 0 & 0 & \dots & 0 \end{bmatrix} \quad [14]$$

$$\Sigma = \begin{bmatrix} -\sigma & \dots & 0 & \eta\sigma & \dots & 0 & (1-\eta)\sigma & \dots & 0 \\ \vdots & -\sigma & \vdots & \vdots & \eta\sigma & \vdots & \vdots & (1-\eta)\sigma & \vdots \\ 0 & \dots & -\sigma & 0 & \dots & \eta\sigma & 0 & \dots & (1-\eta)\sigma \\ 0 & \dots & 0 & -\gamma_a & \dots & 0 & 0 & \dots & 0 \\ \vdots & \ddots & \vdots & \vdots & -\gamma_a & \vdots & \vdots & \ddots & \vdots \\ 0 & \dots & 0 & 0 & \dots & -\gamma_a & 0 & \dots & 0 \\ 0 & \dots & 0 & 0 & \dots & 0 & -\gamma_s & \dots & 0 \\ \vdots & \ddots & \vdots & \vdots & \ddots & \vdots & \vdots & -\gamma_s & \vdots \\ 0 & \dots & 0 & 0 & \dots & 0 & 0 & \dots & -\gamma_s \end{bmatrix} \quad [15]$$

Disease progression parameters. The case fatality rate by age were obtained from Public Health Ontario data (8). Transition rates for the duration of the asymptomatic infectious period and the proportion of symptomatic cases were obtained from COVID-19 epidemiological literature (9–11).

Initial conditions. The point $t = 0$ was chosen to be the day at which the province of Ontario recorded more than 50 cases, March 10th 2020, to reduce the effects of stochasticity in the early case counts. Let the number of observed cases of COVID-19 in age group i on March 10th 2020 be ω_i. We use the age distribution of ω_i to determine the age distribution for $I_a(t) + I_s(t)$. The true number of cases that day is ω_i/α_i, where α_i is the ascertainment rate of cases in group i. Since we do not know the actual number of active cases, $I_{a_i}(t) + I_{s_i}(t)$ at $t = 0$, we assume the number of active cases is equal to the true number of incident cases multiplied by a constant I_0, which is also treated as a model variable to be fitted. Therefore, $I_{s_i}(0) = \eta I_0 \frac{\omega_i}{\alpha_i}$ and $I_{a_i}(0) = (1-\eta) I_0 \frac{\omega_i}{\alpha_i}$. We assumed that $S_i^1(0) = N_i$, so the total number of susceptible, unvaccinated individuals $\sum_{i=1}^{16} S_i^1(0)$ is the population of the region, and $S_i^2(0) = 0, S_i^3(0) = 0, E_i(0) = 0, R_i(0) = 0$ for all i. Lastly, we assumed that at $t = 0$, only 1% of individuals are physical distancing, so $x(0) = 0.01$, and that $D(0) = 0$.

Particle filtering. We calibrated the model with data from Ontario, Canada. Since the workplace closure opening and closing rates, k_1 and k_2, are not coupled with the model, we fit a step function of the form

$$f(t) = \epsilon_W \left(\tanh k_1 (t - t^W_{close}) - \tanh k_2 (t - t^W_{close}) \right)$$

to the "workplaces_percent_change_from_baseline" field of the Google mobility data (12) for the province.

We applied a particle filtering approach using intervals around selected parameters. Intervals used for sampling appear in Table S1. We fit the cumulative cases across all age groups at each day to the number of cases registered by Public Health Ontario on that day (13), and the decrease in contact-hours to the decrease in the "Retail and Recreation" hours recorded by Google mobility (12). The posterior distribution of the parameters was estimated with the approximate Bayesian computation scheme described in (14), with uniform priors and 500 particles, using the KissABC library for the Julia language. The acceptance threshold was chosen to given acceptable variation and evaluation time.

To reduce the size of the parameter space while conducting the particle filtering, we down-sampled the ascertainment and susceptibility vectors to represent two age classes with one ascertainment rate and susceptibility factor, respectively. These resulting vectors of eight real numbers each were interpolated with quadratic polynomials to give sixteen ascertainment rates and susceptibility factors used in the model (see Figures **??**). The ascertainment rate for the youngest four age groups was bounded between 0.05 and 0.2, and ascertainment rate for the oldest age group (75+) was bounded from below by 0.8. We bounded the age-specific susceptibility factors ρ_i between 0.5 and 2. The phase of the seasonal susceptibility was chosen to be -30, which corresponds to a peak in early February of each year if $s < 0$, or early august if $s > 0$ (depending on the exact start date of the simulation).

Optimized vaccination strategy. We compared four vaccination strategies in our baseline analysis: uniform vaccination, oldest first, youngest first, and the contact-matrix based strategy. To construct a strategy that is better than these four, we began a local optimization with each of these aforementioned strategies as initial points. In particular, we used the method of moving asymptotes (15) for constrained nonlinear local optimization available in NLOpt (16), a popular nonlinear optimization library. The method was run until convergence with each of the initial points, and the best of the resulting local optimums taken. Although a global optimization algorithm is potentially able to find better strategies given enough time, we found that for reasonable execution times, the multistart method we used here achieves similar optimal solutions. The objective function ran the model for five years, and minimized the total number of deaths over that time.

Table S1. Parameter definitions, values, particle filtering ranges, and sources.

Parameter	Meaning	Value [Range]	Source
N_i	Population in age group i	$0-4$: 790169; $5-9$: 789190 $10-14$: 790803; $15-19$: 887072 $20-24$: 1003052; $25-29$: 1015105 $30-34$: 1009090; $35-39$: 969949 $40-44$: 926440; $45-49$: 938990 $50-54$: 1027557; $55-59$: 10416495 $60-64$: 892016; $65-69$: 741824 $70-74$: 557203; $75+$: 204431	(17), interpolated
μ_i	COVID-19 case fatality rate in age group i	$0-4$: 0.002; $5-9$: 0.001 $10-14$: 0.0005; $15-19$: 0.0005 $20-24$: 0.0010; $25-29$: 0.002 $30-34$: 0.0031; $35-39$: 0.0048 $40-44$: 0.0078; $45-49$: 0.0135 $50-54$: 0.0253; $55-59$: 0.0455 $60-64$: 0.0784; $65-69$: 0.1378 $70-74$: 0.2623; $75+$: 0.5815	(8), interpolated
C_{ij}	contact rate between class i and j	see Supp. Methods	(18)
R_0	basic reproduction rate of infection	calibrated, $[1.5, 2.5]$	(12, 13, 19)
r	probability of transmission per contact	derived from next generation matrix	(7)
σ	inverse of latent period	calibrated, $[0.3, 2.0]$	(9–13)
γ_a	inverse of infectious period for asymptomatic individuals	0.25/day	(9–11)
γ_s	inverse of infectious period for symptomatic individuals	calibrated, $[0.0, 0.05]$	(9–13)
α_i	Ascertainment rate of class i	calibrated, $[0.01, 1.0]$	see Supp. Methods
ρ_i	Susceptibility of class i	calibrated, $[0.5, 2.0]$	see Supp. Methods
η	fraction of symptomatic infections	0.15	(20)
ϵ_P	efficacy of physical distancing	calibrated, $[0.3, 0.9]$	(12, 13)
κ	social learning rate	calibrated, $[1000, 16000]$	(12, 13)
s	seasonality	calibrated, $[-0.3, 0.3]$	(12, 13)
ϕ	seasonality phase	-30 days	see Supp. Methods
v_i	Vaccine efficacy for individuals in group i	90%	(21)
I_0	Initial ratio of active cases to incident cases	calibrated, $[1, 3]$	(12, 13)
ψ_i	Number of vaccines allocated for individuals in group i each day	varied by scenario	
T	Threshold in active reported cases for school/workplace closure	varied by scenario	
k_1	Workplace shutdown rate	0.31432	fitted, see Supp. Methods
k_2	Workplace opening rate	0.0056	fitted, see Supp. Methods
c	Incentive not to distance	calibrated,$[0.0, 0.5]$	(12, 13)
p_{ul}	social heterogeneity parameter	calibrated, $[0.00, 0.05]$	(12, 13)
t^s_{close}	School shutdown date	March 14th, 2020	(22)
t^s_{open}	School opening date	September 17th, 2020	(23)
t^w_{close}	Work shutdown date	March 17th, 2020	(24)
t^w_{open}	Work opening date	June 12th, 2020	(24)
ϵ_w	Work shutdown effectiveness	0.86	fitted, see Supp. Methods

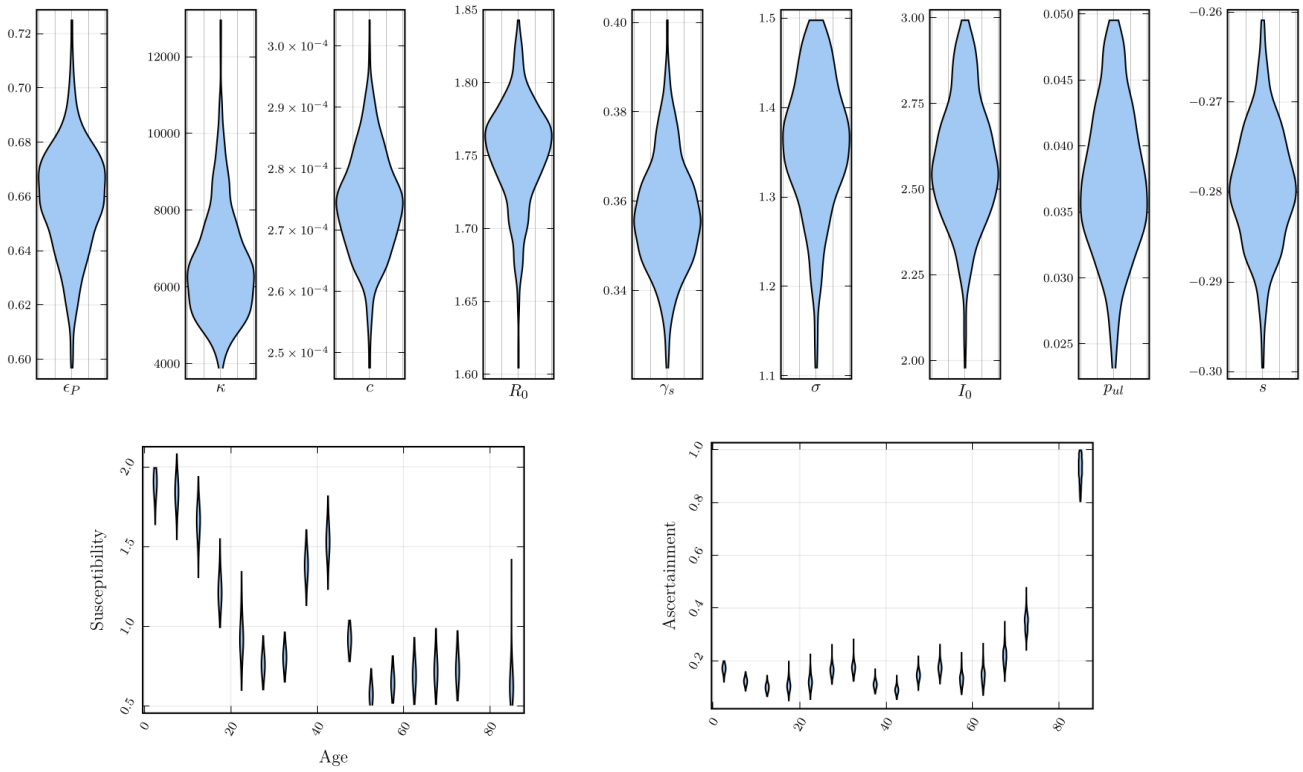

Fig. S1. Posterior distributions on inferred parameters for age-specific susceptibility (lower left), age-specific ascertainment (lower right) and non-age structured model parameters (top) for baseline model. See Model overview and Supplementary Methods for details.

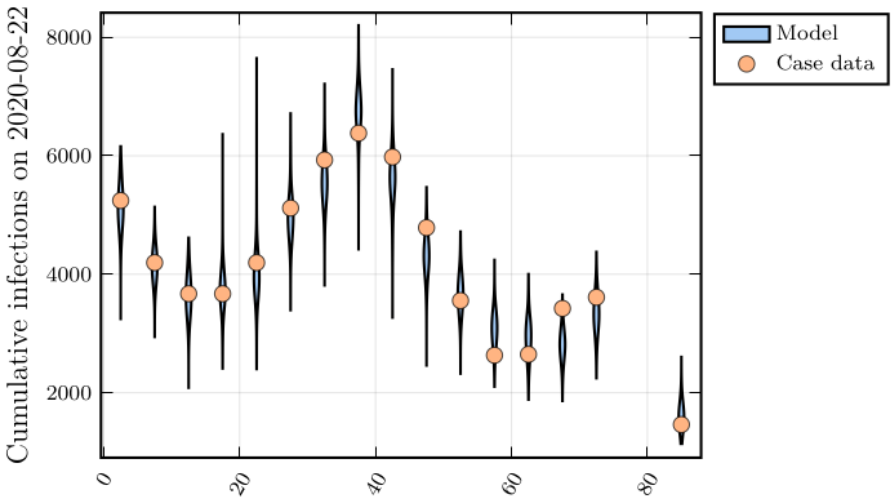

Fig. S2. Empirical data of cumulative infections due to COVID-19 by age and posterior predictions. See Model overview and Supplementary Methods for details.

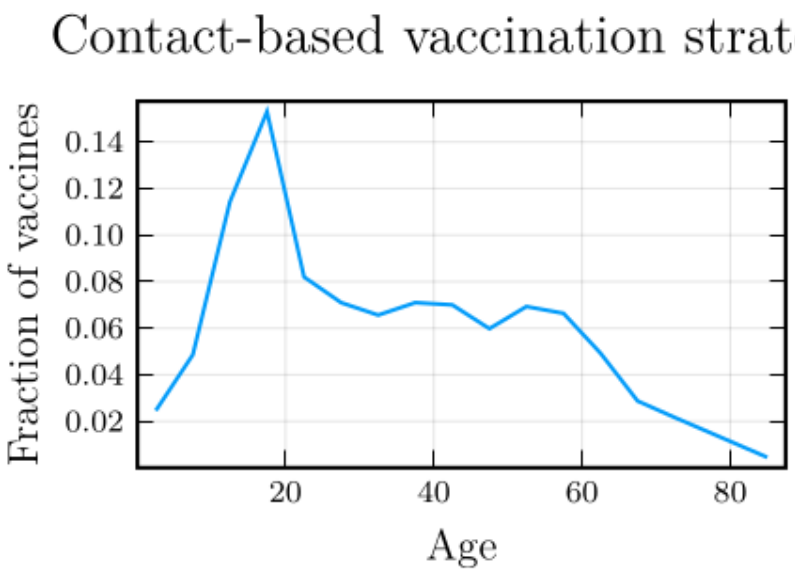

Fig. S3. Age distribution of vaccination under the contact-based strategy. See Model overview and Supplementary Methods for details.

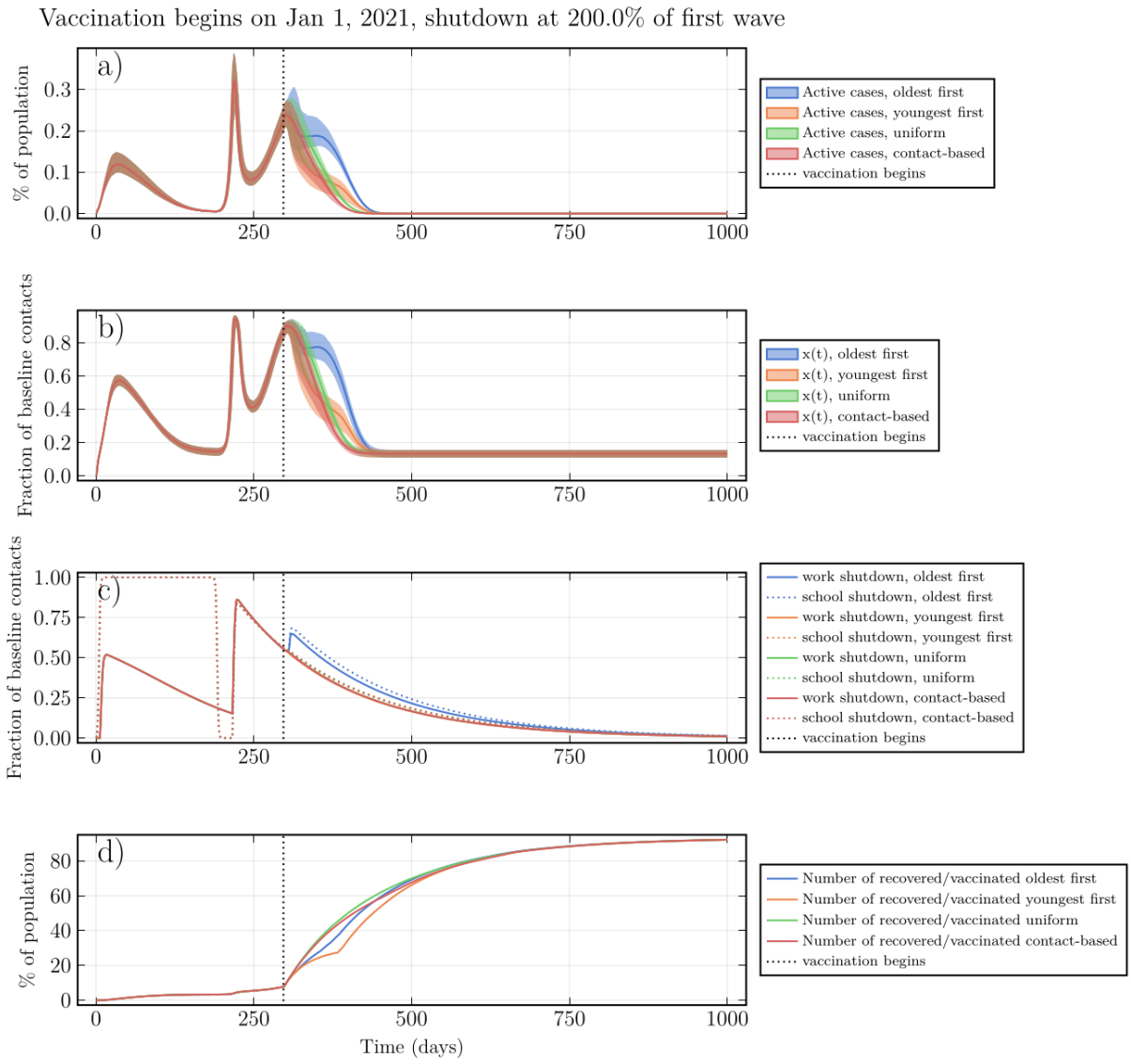

Fig. S4. Social and epidemic dynamics for early vaccine availability and high vaccination rate. (a) Active ascertained COVID-19 cases, (b) proportion x of the population practicing NPIs, (c) Intensity of school and workplace closure, (d) percentage of population with natural or vaccine-derived immunity versus time. $T = 2.0$, $\psi_0 = 4.5\%$ per week, vaccine available in January 2021. Other parameters are in Table S1.

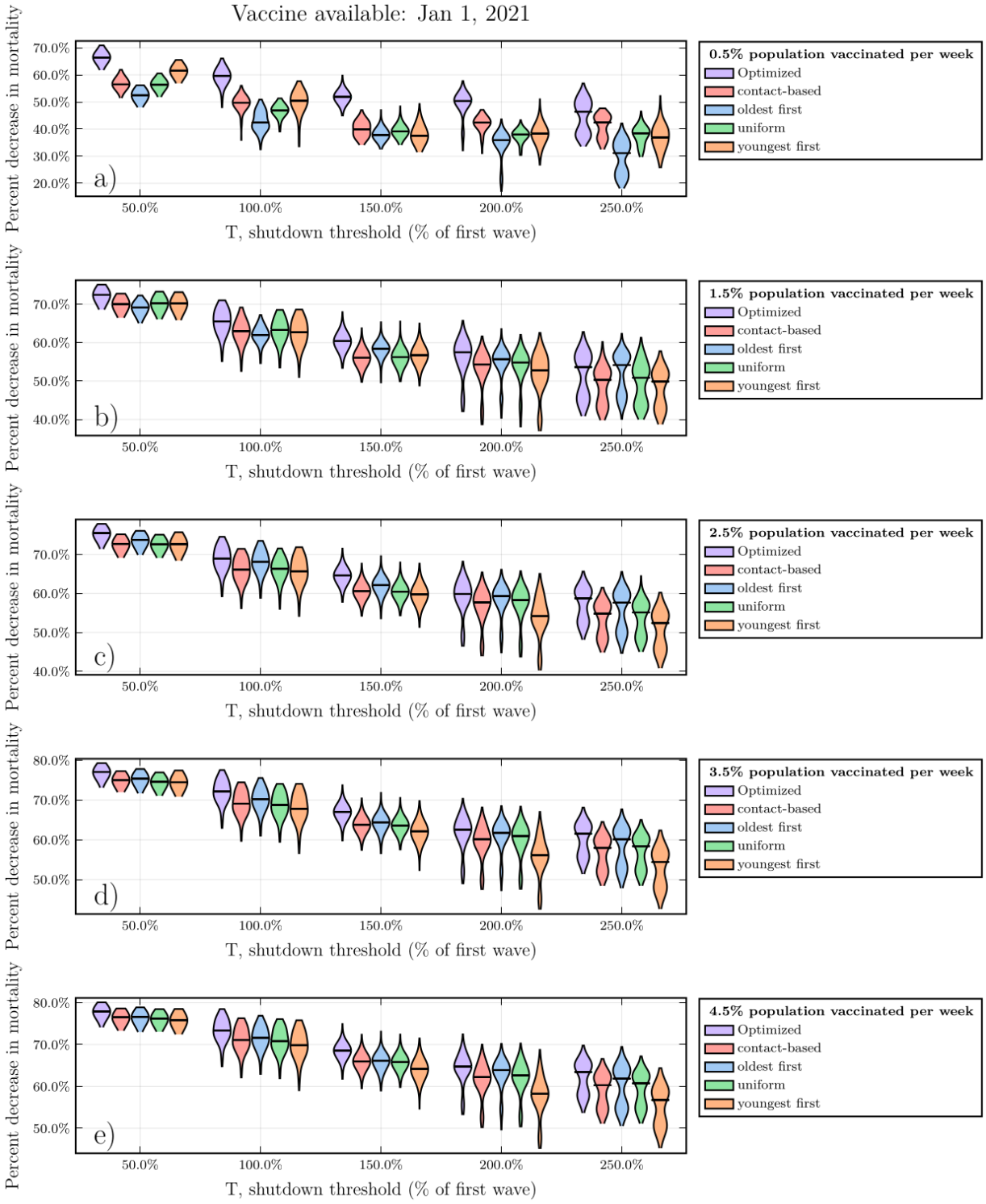

Fig. S5. Mortality reductions under various values of T and ψ_0, January vaccine availability. Violin plots of the percent reduction in mortality under the four vaccine strategies, relative to no vaccination, as a function of the vaccination rate ψ_0, for January 2021 availability. Horizontal lines represent median values of posterior model projections. Other parameter values in Table S1.

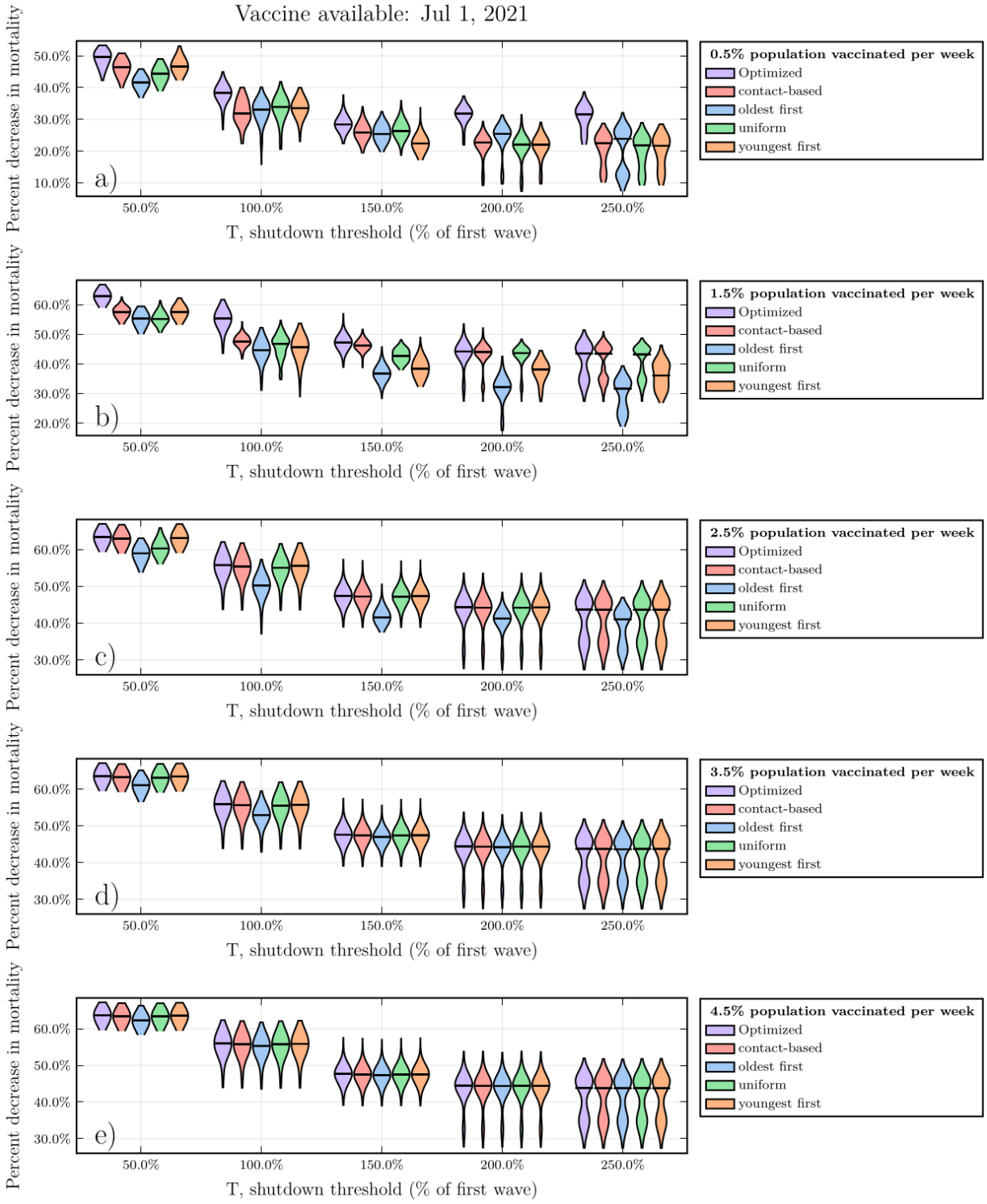

Fig. S6. Mortality reductions under various values of T and ψ_0, July vaccine availability. Violin plots of the percent reduction in mortality under the four vaccine strategies, relative to no vaccination, as a function of the vaccination rate ψ_0, for July 2021 availability. Horizontal lines represent median values of posterior model projections. Other parameter values in Table S1.

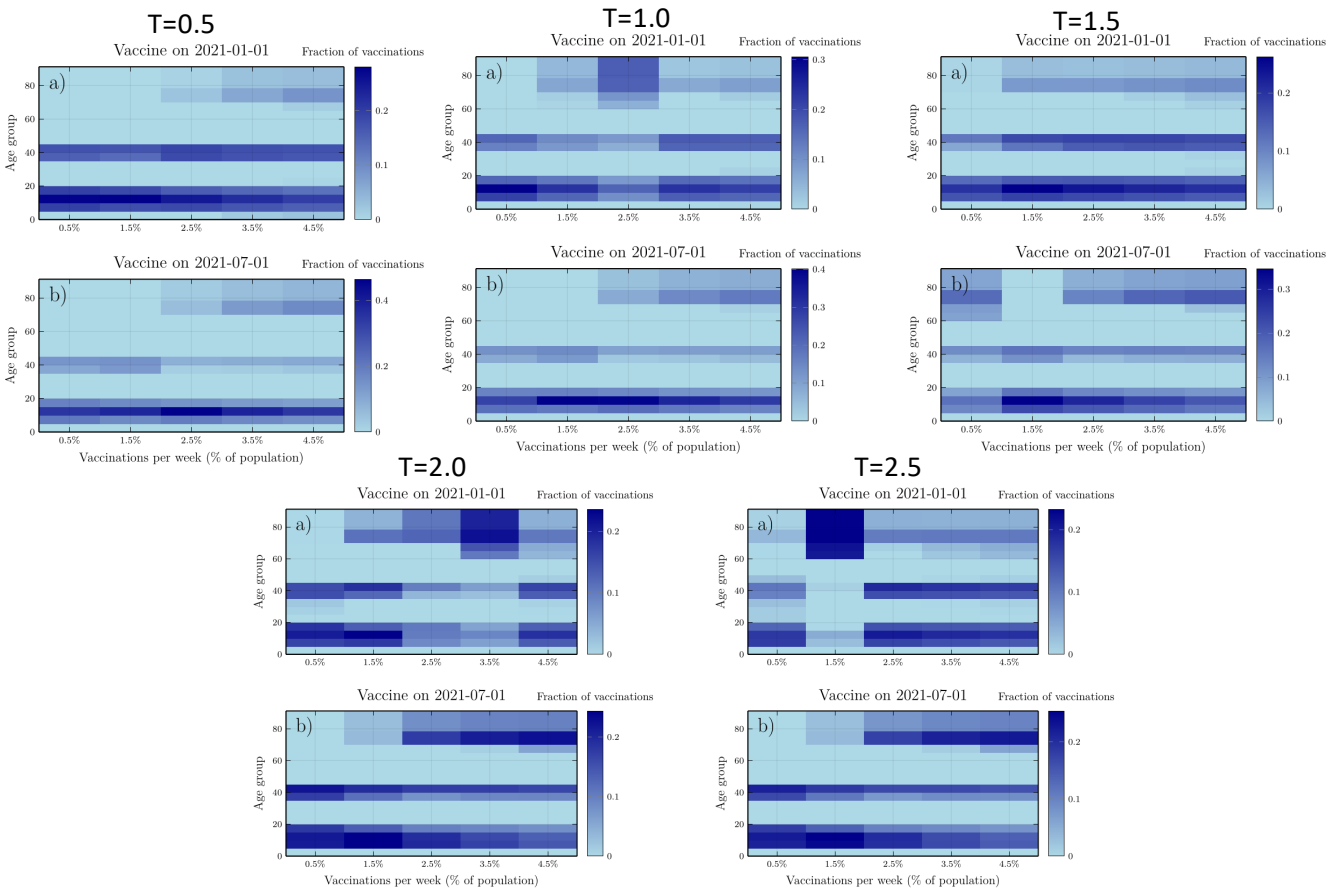

Fig. S7. Age distribution of vaccine under the optimal strategy, for various values of T and ψ_0 (horizontal axis), for (a) January and (b) July 2021 vaccine availability.

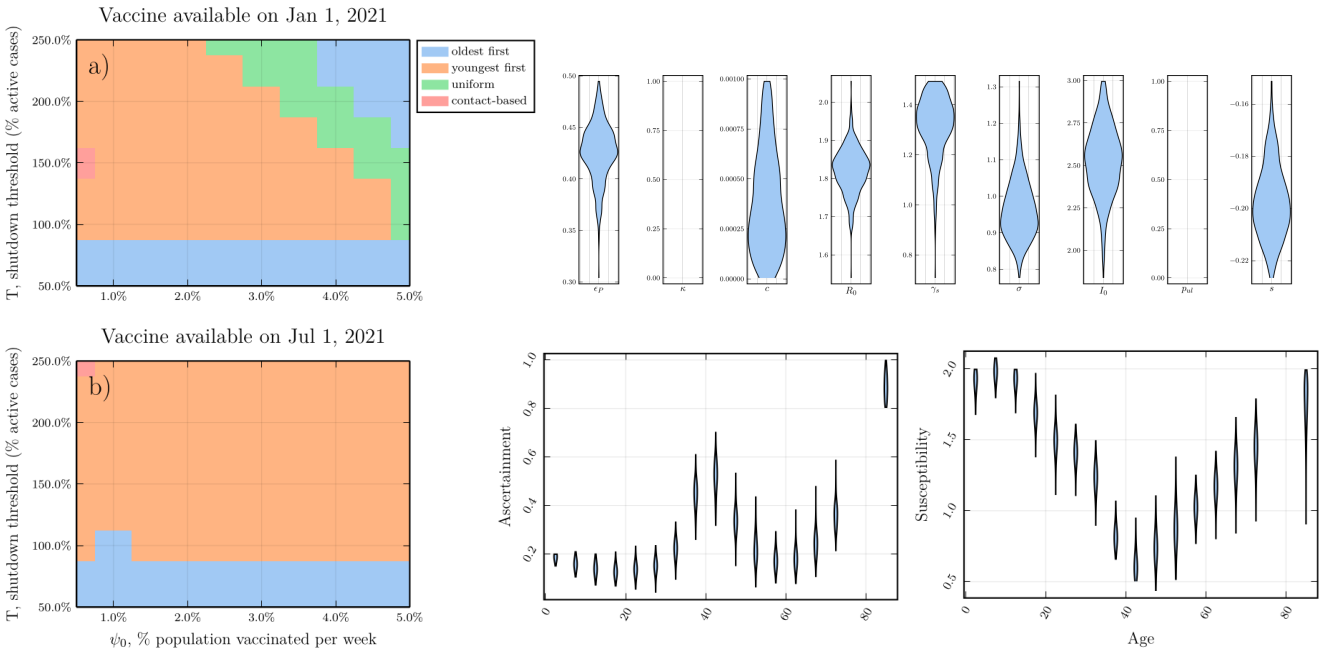

Fig. S8. Sensitivity analysis for the scenario where population adherence to NPIs is constant over time. Subpanels are parameter planes for January and July availability showing the vaccination strategy that reduces COVID-19 mortality the most as a function of T and ψ_0 (left) and the corresponding posterior parameter distributions for the refitted parameters (right). Other parameter values as in Table S1.

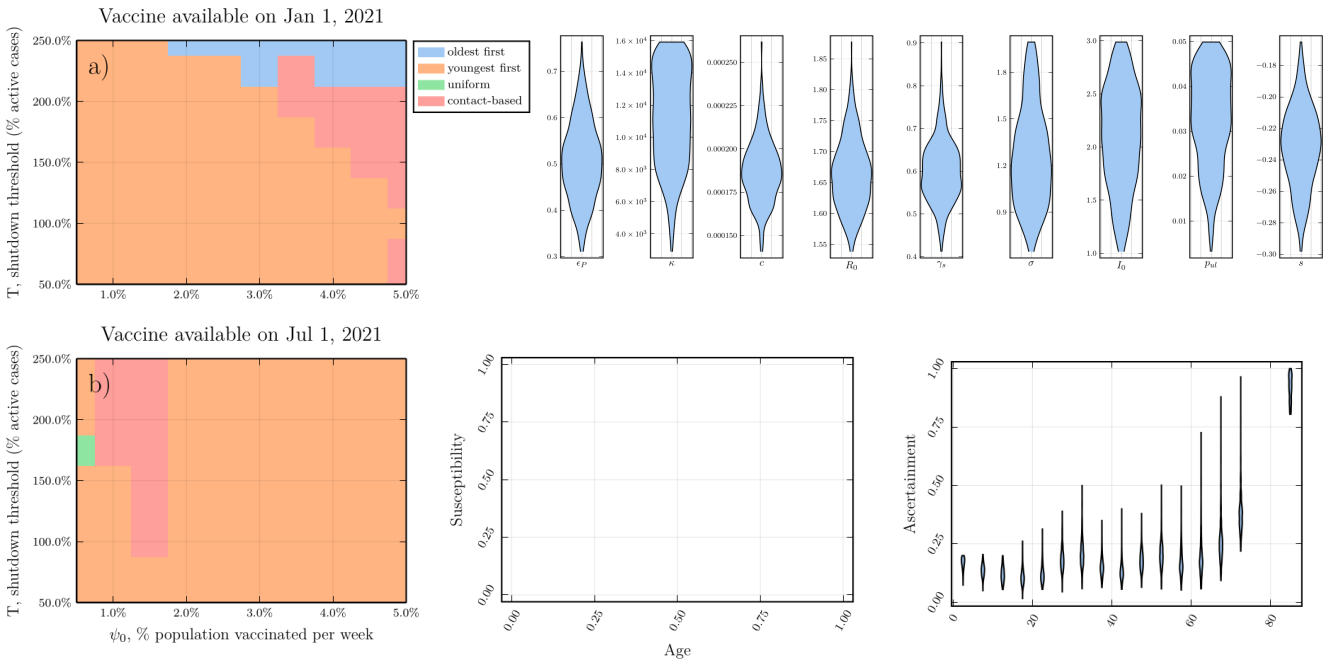

Fig. S9. Sensitivity analysis for the scenario where infection susceptibility is constant across ages. Subpanels are parameter planes for January and July availability showing the vaccination strategy that reduces COVID-19 mortality the most as a function of T and ψ_0 (left) and the corresponding posterior parameter distributions for the refitted parameters (right). Other parameter values as in Table S1.

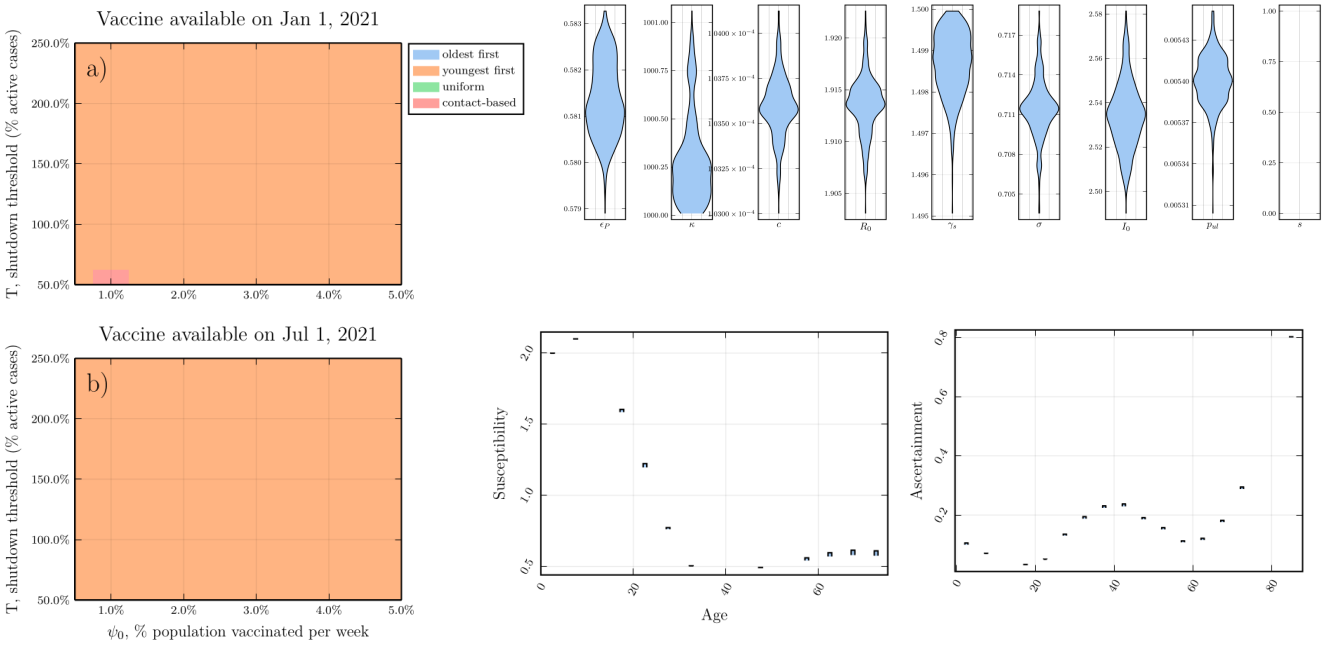

Fig. S10. Sensitivity analysis for the scenario in the absence of seasonality. Subpanels are parameter planes for January and July availability showing the vaccination strategy that reduces COVID-19 mortality the most as a function of T and ψ_0 (left) and the corresponding posterior parameter distributions for the refitted parameters (right). Other parameter values as in Table S1.

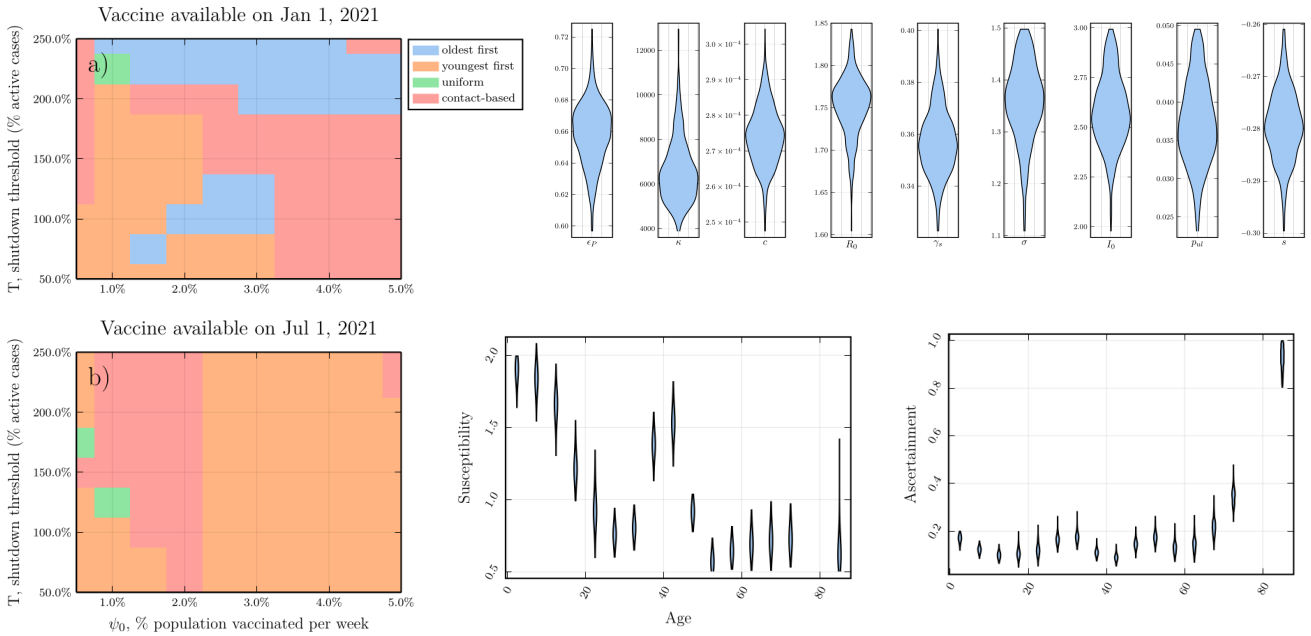

Fig. S11. Sensitivity analysis for the scenario where vaccine efficacy is 50% in older individuals and 90% for everyone else. Subpanels are parameter planes for January and July availability showing the vaccination strategy that reduces COVID-19 mortality the most as a function of T and ψ_0 (left) and the corresponding posterior parameter distributions for the refitted parameters (right). Other parameter values as in Table S1.

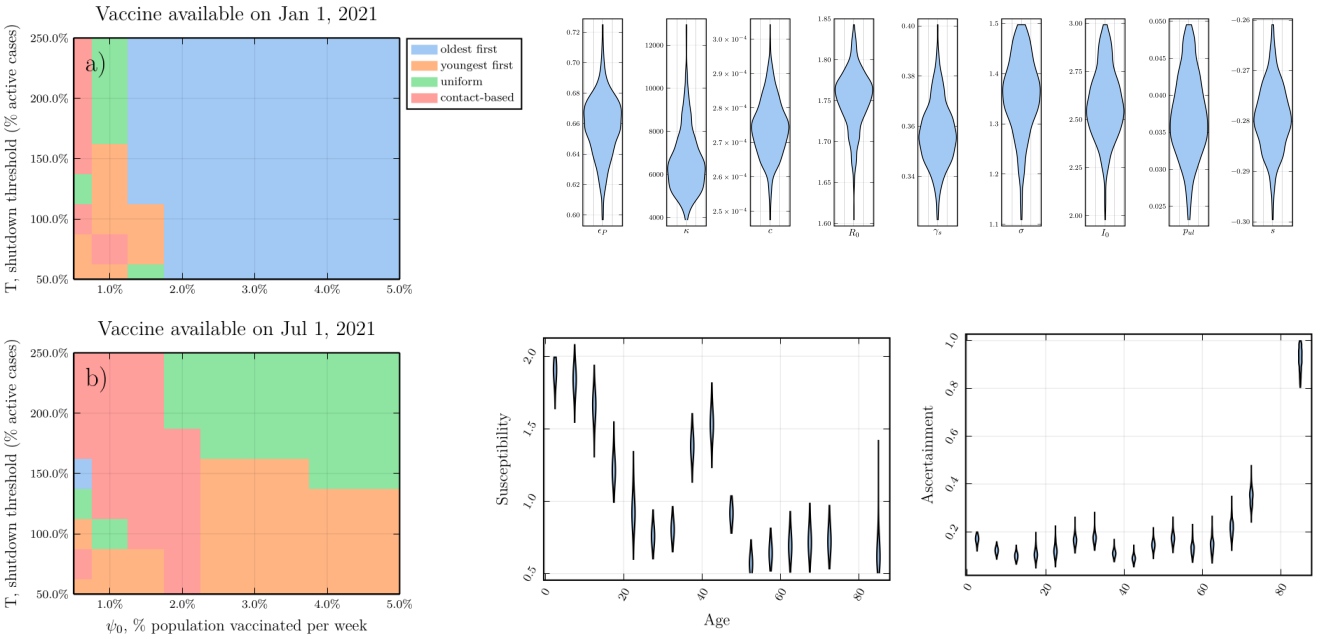

Fig. S12. Sensitivity analysis for the scenario of increased efficacy of NPIs in the second wave to account for more widespread use of masks. Subpanels are parameter planes for January and July availability showing the vaccination strategy that reduces COVID-19 mortality the most as a function of T and ψ_0 (left) and the corresponding posterior parameter distributions for the refitted parameters (right). Other parameter values as in Table S1.

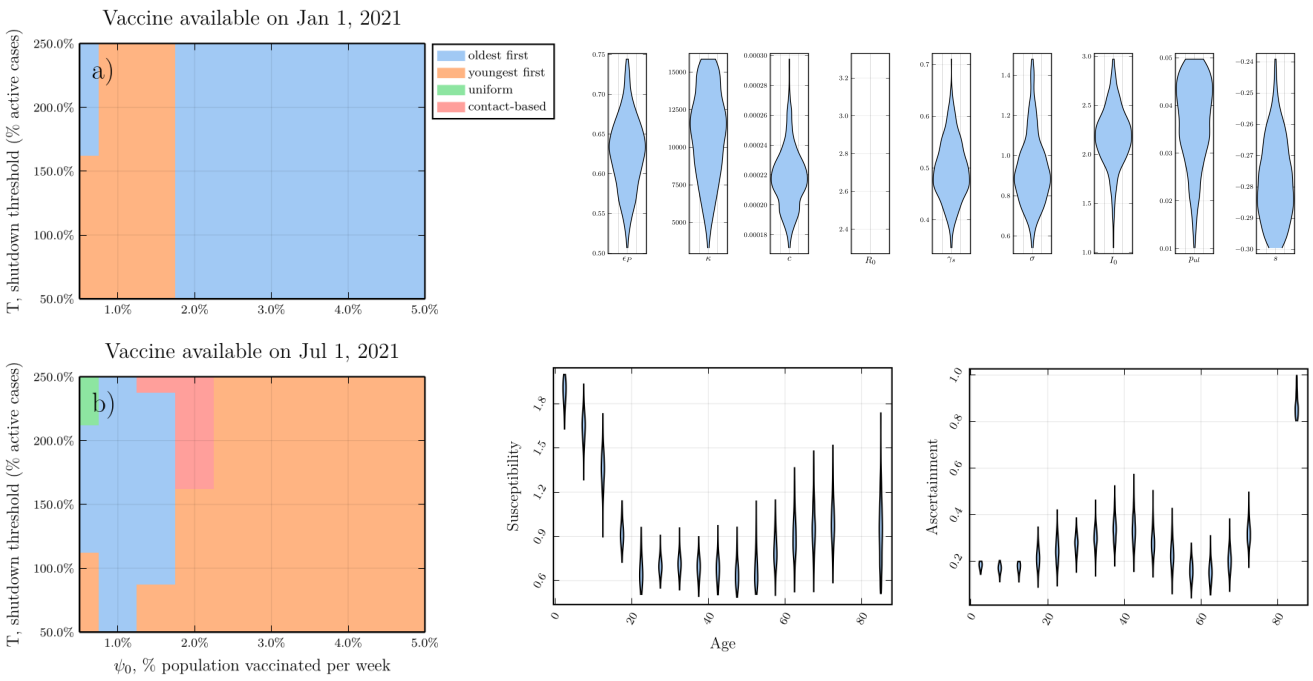

Fig. S13. Sensitivity analysis for the scenario where $R_0 = 2.3$. Subpanels are parameter planes for January and July availability showing the vaccination strategy that reduces COVID-19 mortality the most as a function of T and ψ_0 (left) and the corresponding posterior parameter distributions for the refitted parameters (right). Other parameter values as in Table S1.

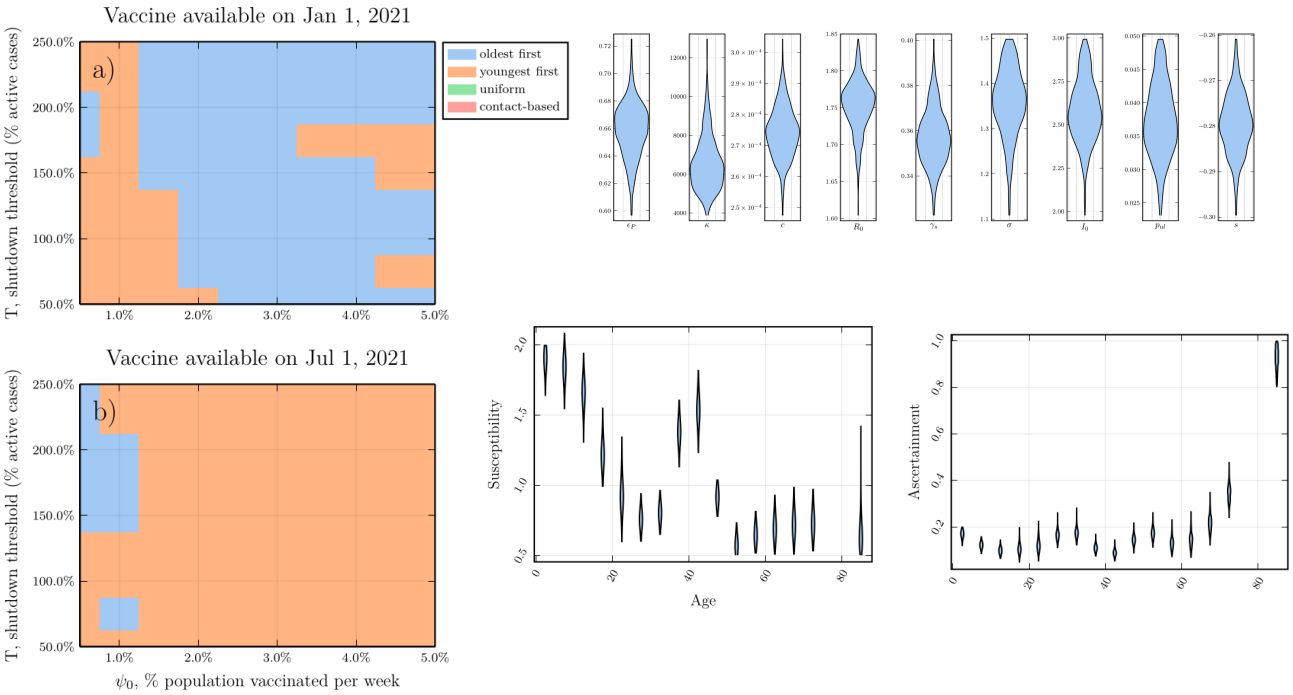

Fig. S14. Sensitivity analysis for the scenario of 50% vaccine efficacy for everyone. Subpanels are parameter planes for January and July availability showing the vaccination strategy that reduces COVID-19 mortality the most as a function of T and ψ_0 (left) and the corresponding posterior parameter distributions for the refitted parameters (right). Other parameter values as in Table S1.

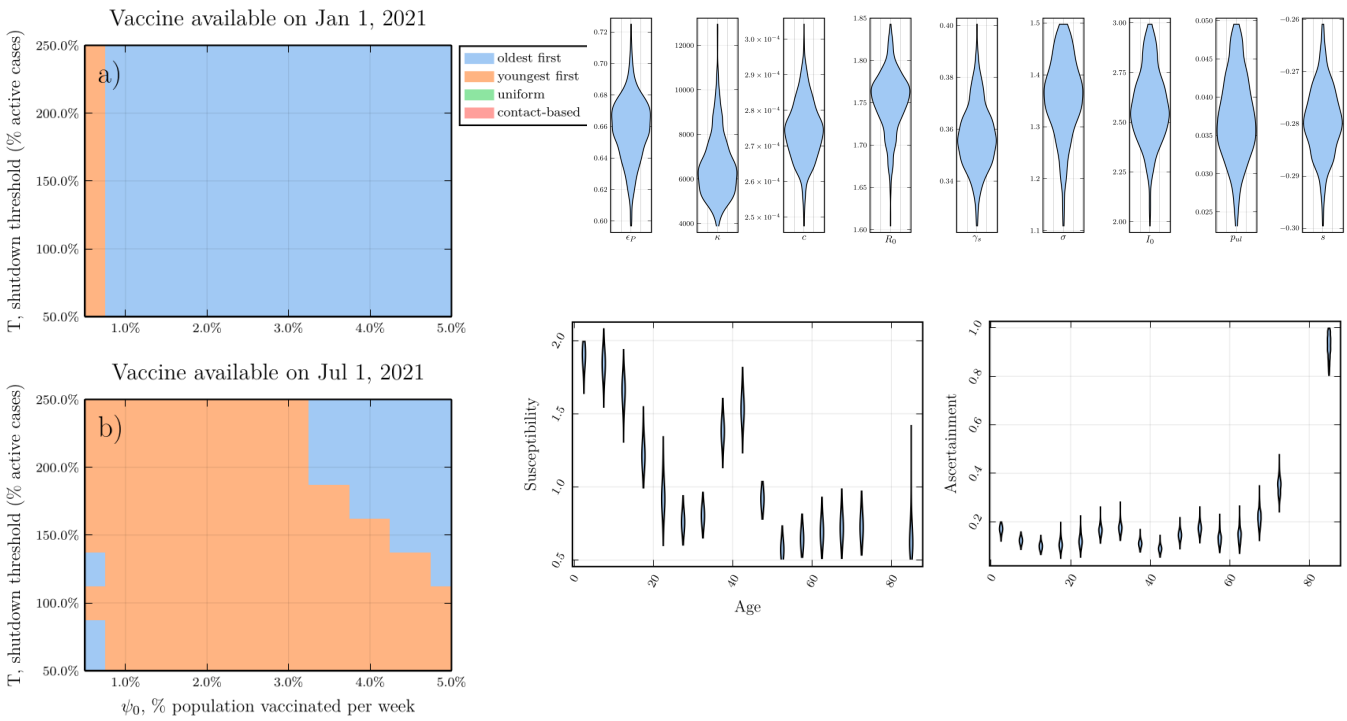

Fig. S15. Sensitivity analysis for the scenario when individuals are tested for seropositivity before being administered a vaccine. Subpanels are parameter planes for January and July availability showing the vaccination strategy that reduces COVID-19 mortality the most as a function of T and ψ_0 (left) and the corresponding posterior parameter distributions for the refitted parameters (right). Other parameter values as in Table S1.

Supplementary Appendix References

1. CT Bauch, Imitation dynamics predict vaccinating behaviour. *Proc. Royal Soc. B: Biol. Sci.* **272**, 1669–1675 (2005).
2. C Innes, M Anand, CT Bauch, The impact of human-environment interactions on the stability of forest-grassland mosaic ecosystems. *Sci. reports* **3**, 1–10 (2013).
3. VA Thampi, M Anand, CT Bauch, Socio-ecological dynamics of caribbean coral reef ecosystems and conservation opinion propagation. *Sci. reports* **8**, 1–11 (2018).
4. CT Bauch, S Bhattacharyya, Evolutionary game theory and social learning can determine how vaccine scares unfold. *PLoS Comput. Biol* **8**, e1002452 (2012).
5. T Oraby, V Thampi, CT Bauch, The influence of social norms on the dynamics of vaccinating behaviour for paediatric infectious diseases. *Proc. Royal Soc. B: Biol. Sci.* **281**, 20133172 (2014).
6. E Zagheni, et al., Using time-use data to parameterize models for the spread of close-contact infectious diseases. *Am. journal epidemiology* **168**, 1082–1090 (2008).
7. O Diekmann, J Heesterbeek, MG Roberts, The construction of next-generation matrices for compartmental epidemic models. *J. Royal Soc. Interface* **7**, 873–885 (2010).
8. Ontario Agency for Health Protection and Promotion (Public Health Ontario), COVID-19 case fatality, case identification, and attack rates in ontario (https://www.publichealthontario.ca/-/media/documents/ncov/epi/2020/06/COVID19-epi-case-identification-age-only-template.pdf?la=en) (2020).
9. H Nishiura, NM Linton, AR Akhmetzhanov, Serial interval of novel coronavirus (COVID-19) infections. *Int. journal infectious diseases* (2020).
10. SA Lauer, et al., The incubation period of coronavirus disease 2019 (COVID-19) from publicly reported confirmed cases: estimation and application. *Annals internal medicine* (2020).
11. L Tindale, et al., Transmission interval estimates suggest pre-symptomatic spread of COVID-19. *medRxiv* (2020).
12. Google, Inc., COVID-19 community mobility reports (2020) Available at https://www.google.com/{COVID}19/mobility/.
13. Treasury Board Secretariat of Ontario, Confirmed positive cases of COVID-19 in Ontario (2020) Available at https://data.ontario.ca/dataset/confirmed-positive-cases-of-{COVID}-19-in-ontario/resource/455fd63b-603d-4608-8216-7d8647f43350.
14. BM Turner, PB Sederberg, Approximate Bayesian computation with differential evolution. *J. Math. Psychol.* **56**, 375–385 (2012).
15. K Svanberg, A class of globally convergent optimization methods based on conservative convex separable approximations. *SIAM journal on optimization* **12**, 555–573 (2002).
16. SG Johnson, The NLopt nonlinear-optimization package (2020) Available at http://github.com/stevengj/nlopt.
17. Statistics Canada, Census profile, 2016 census, https://www12.statcan.gc.ca/, accessed 25 september 2020 (year?).
18. K Prem, et al., Projecting contact matrices in 177 geographical regions: an update and comparison with empirical data for the COVID-19 era. *medRxiv* (2020).
19. J Hilton, MJ Keeling, Estimation of country-level basic reproductive ratios for novel coronavirus (COVID-19) using synthetic contact matrices. *medRxiv* (2020).
20. K Mizumoto, K Kagaya, A Zarebski, G Chowell, Estimating the asymptomatic proportion of coronavirus disease 2019 (COVID-19) cases on board the diamond princess cruise ship, yokohama, japan, 2020. *Eurosurveillance* **25**, 2000180 (2020).
21. WH Organization, Who target product profiles for COVID-19 vaccines, https://www.who.int/who-documents-detailredirect/ who-target-product-profiles-for-COVID-19-vaccines, accessed 25 september 2020 (2020).
22. Globalnews Canada, Coronavirus: All publicly funded schools in ontario closing for 2 weeks due to COVID-19. (2020) https://globalnews.ca/news/6668240/coronavirus-ontario-schools-closed/.
23. Globalnews, The dates and staggered starts for all GTA schools. (2020) https://globalnews.ca/news/

6668240/coronavirus-ontario-schools-closed/.
24. Provincial government of Ontario, Canada, Reopening ontario in stages (2020) Available at https://www.ontario.ca/page/reopening-ontario-stages.